

BL33XU (TOYOTA)

1. Introduction

BL33XU was constructed in FY2009 and is operated by Toyota Central R&D Labs. This beamline was built to realize high-speed X-ray absorption fine structure (XAFS) for *operando* analysis and three-dimensional X-ray diffraction (3DXRD), which were techniques unavailable at SPring-8 in 2009. Small-angle X-ray scattering (SAXS), X-ray diffraction with a multi-axis goniometer, X-ray computed tomography/laminography techniques were installed this decade, and two technical groups as “*operando* analysis with multi probe” and “non-destructive three-dimensional structural analysis” were established (Fig. 1). Here, the current status and recent technological progress of the beamline are reported.

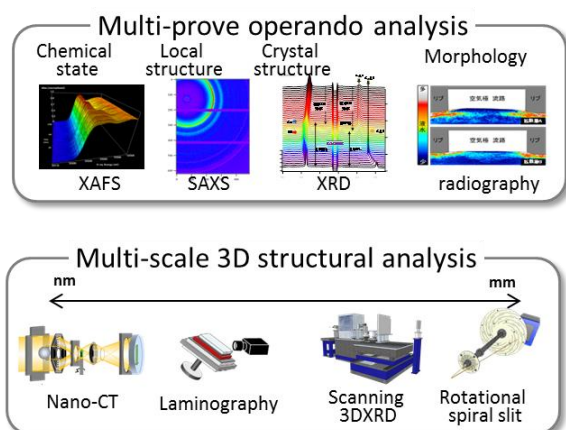


Fig. 1. Analysis techniques at BL33XU.

2. Outline of the beamline

2-1. Beamline layout

The TOYOTA beamline is a medium-length beamline, which has an experimental facility building outside the storage ring building. An

optical hutch is located in the storage ring building, and three experimental hutches, chemical preparation room, operation area, and office room constitute the experimental facility building.

Figure 2 shows the layout of the optical components of this beamline. The beamline has two optics with different types of monochromators. Optics 1 consists of a horizontal mirror pair (M1 and M2) in the optics hutch, compact monochromators (C-Mono) with channel-cut crystals, and a vertical mirror pair (M3 and M4) in experimental hutch 1. The beam size at the sample position is variable from 0.1 mm to 18 mm using bendable mirrors (M2, M3, and M4). These optics are mainly used for high-speed X-ray absorption fine structure (XAFS) analysis. Optics 2 is composed of a standard SPring-8 double-crystal monochromator, vertical mirror pair (M4 and M5), and Kirkpatrick-Baez mirror (KBM). A microbeam with 1 μm square at 50 keV is available at experimental hutch 3.

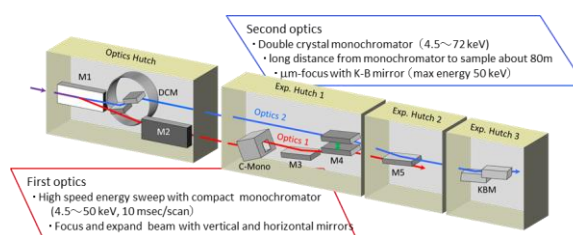


Fig. 2. Optics in BL33XU.

2-2. Analysis techniques

(1) Quick-scanning XAFS system

The system features high-speed XAFS measurements using a specially designed spectrometer. With this configuration, an XAFS spectrum can be acquired with a temporal resolution

of 10 ms by rotationally oscillating a servomotor-driven channel-cut Si(111) or Si(220) crystal at 50 Hz^[1]. The measurable energy range covers from 4.5 keV to 45 keV. A high signal-to-noise ratio is achieved by a high-speed 24-bit analog-to-digital converter (PXI-5922; National Instruments).

Various *in situ* measurement techniques have been developed. These include simultaneous XAFS and XRD measurements of positive and negative electrodes of lithium-ion batteries during charging and discharging^[2].

(2) SAXS

The camera length can be selected from tens of centimeters to 4.5 meters. The detector is PILATUS 300K (Dectris). Several *in situ* observation techniques have been developed. For example, the structure evolution of resins while injection molding can be analyzed^[3].

(3) XRD

A multi-axis goniometer head (1001; HUBER) is equipped. A newly developed rotating and revolving spiral slits system can detect diffraction peaks from any microregion in the specimen with a two-dimensional detector (*e.g.*, PILATUS). The slit shapes are designed so that the gauge volume viewed through the slits is independent of the diffraction angle^[4]. In addition, revolving slits allow diffraction spectra to be acquired at larger angles^[5].

(4) Scanning 3DXRD

The scanning 3DXRD method was developed for non-destructive analysis of practical metallic materials with hundreds of grains in the observation region. This technique is more sensitive than conventional 3DXRD techniques, which can analyze several tens of grains. In 2013, this method was validated, and high-resolution analysis using a

high-energy microbeam was demonstrated in 2015^[6]. Not only the average properties of each grain but also special distribution of the properties in the grain can be acquired. Additionally, this technique can provide the strain distribution in the crystal rotation.

(5) Tomography and laminography

X-ray computed tomography (CT) and laminography techniques were introduced to meet the growing needs of high-resolution, non-destructive structural analysis of materials. A resolution of less than 1 μm was achieved for the CT method, and $\sim 1\text{-}\mu\text{m}$ resolution was recently obtained in the laminography method. In addition, an imaging CT system introduced in 2017 achieved a resolution of $\sim 100\text{ nm}$.

3. Recent technological progress

3-1. *In situ* XRS for lithium-ion batteries^[7]

Although the TOYOTA beamline has advanced *in situ / operando* analysis techniques, it can only analyze elements heavier than titanium with X-ray absorption spectroscopy. To analyze the chemical state of light elements, X-ray Raman scattering (XRS) system was installed into the beamline in 2017. XRS is an energy loss spectroscopy that utilizes hard X-rays as a bulk sensitive probe to provide information equivalent to soft X-ray absorption spectroscopy (XAS) and electron energy loss spectroscopy (EELS).

In the negative electrode of a lithium-ion battery, the crystal structure of graphite changes from LiC_6 to LiC_{12} , then to pure graphite upon discharging. This chemical state change was investigated using an XRS technique. Because a lithium-ion battery consists of many carbon-containing materials such as a separator, electrolyte, and laminate film

packing the battery, the technique must be able to detect only signals from the negative electrode. Figure 3 shows a schematic image of the designed pouch cell and a diagram of the analysis region in XRS measurements. The graphite electrode was

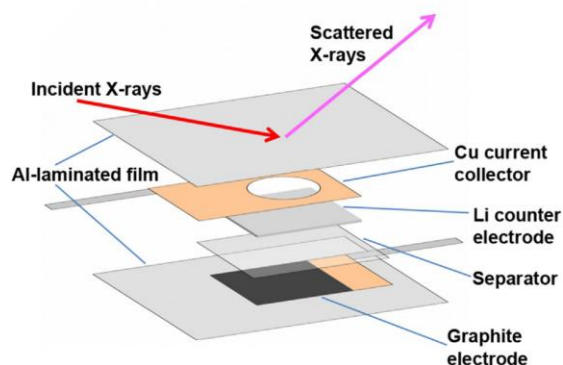


Fig. 3. Schematic of the pouch cell designed for *in situ* XRS measurements [7].

about 100- μm thick. The X-ray beam was vertically focused to approximately 24 μm and was incident on the cell with an angle of 5° . The acceptance width of the analyzer crystal along the X-ray beam direction was about 1.5 mm. The analysis region of XRS was contained within the negative electrode by adjusting the vertical position of the cell. Lithium was used for the counter electrode. The phase of the graphite electrode was controlled by the voltage. Prior to the XRS measurements, the cell was charged to 0.005 V, and the expected graphite state was LiC_6 . After a measurement at 0.005 V, the cell was discharged to 0.12 V and 2 V, where the graphite should be LiC_{12} and fully delithiated graphite, respectively. Figure 4 shows the C K-edge XRS spectra of the graphite electrode at cell voltages of 0.005 V, 0.12 V, and 2 V. The peak at ~ 285.5 eV corresponds to the transition from the $1s$ to π^* state, and the broad feature at ~ 290 eV is the $1s$ to σ^* transition. Two obvious changes occur

upon discharging (*i.e.*, delithiation of graphite electrode). The peak at 285.5 eV increases and the onset peak at 290 eV shifts to a higher energy. These changes are consistent with previous reports from several groups using *ex situ* XRS spectroscopy, soft XAS, and EELS. These results confirm that this measurement is evaluating the change of the graphite electrode.

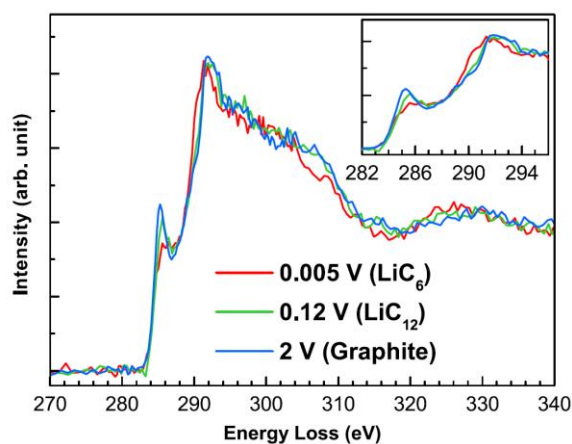


Fig. 4. Comparison of the C K-edge XRS spectra of the graphite electrode at cell voltages of 0.005 V, 0.12 V, and 2 V, corresponding to LiC_6 , LiC_{12} , and fully delithiated graphite, respectively. Inset is an enlargement of the near edge region [7].

3-2. Non-destructive crystal orientation mapping of carbon steel by scanning 3DXRD [8]

A scanning 3DXRD technique developed at BL33XU measured non-destructive crystal orientation mapping of a cold rolled steel sheet. This technique can analyze practical steel materials [9]. Cold rolled steel, however, consists of a single micro-structure as ferrite. Thus, this technique was applied to carbon steel, which consists of ferrite and perlite microstructure.

Commercial carbon steel S35C and S45C were used

as samples. S45C contains more carbon than S35C and has a higher percentage of perlite. The measurement procedure was the same as before. However, the system had issues distinguishing between ferrite and perlite in carbon steel. Perlite grains consist of micro crystallites in the α -phase and θ -phase, while ferrite grains are bigger and consist of the α -phase only. Because the present scanning 3DXRD system cannot detect diffracted X-rays from perlite grains, it is difficult to determine the grain boundary position between perlite and ferrite accurately. To determine the grain boundary from the diffraction intensity from the ferrite grain only, a threshold intensity, which was determined from the diffraction intensity at the boundary between ferrite grains in cold rolled steel, was applied to determine the boundary of ferrite grains. Figure 5 shows the crystal orientation maps of S35C and S45C. The colored and white areas represent ferrite grains and perlite grains, respectively.

This work was supported by JSPS JP26870932.

Kazuhiko Dohmae

Toyota Central R&D Labs.

References:

- [1] T. Nonaka et al, *Rev. Sci. Instrum.* **83**, (2012) 083112.
- [2] T. Tanabe et al, *SPring-8 experiment summary report*, 2015B7001.
- [3] M. Harada et al, *SPring-8 experiment summary report*, 2015A7003, 2015B7003. 7012.
- [4] H. Kimura et al, *SPring-8 experiment summary report*, 2014A7012, 2015B7012.
- [5] H. Kimura et al, *SPring-8 experiment summary report*, 2015B7012.
- [6] Y. Hayashi et al, *SPring-8 experiment summary report*, 2017A7002, 2017B7002.
- [7] T. Nonaka et al, *J. of Power Sources*, **419** (2019) 203.
- [8] Y. Hayashi et al., *SPring-8 experiment summary report*, 2018A7002.
- [9] Y. Hayashi et al., *SPring-8 experiment summary report*, 2017B7002.

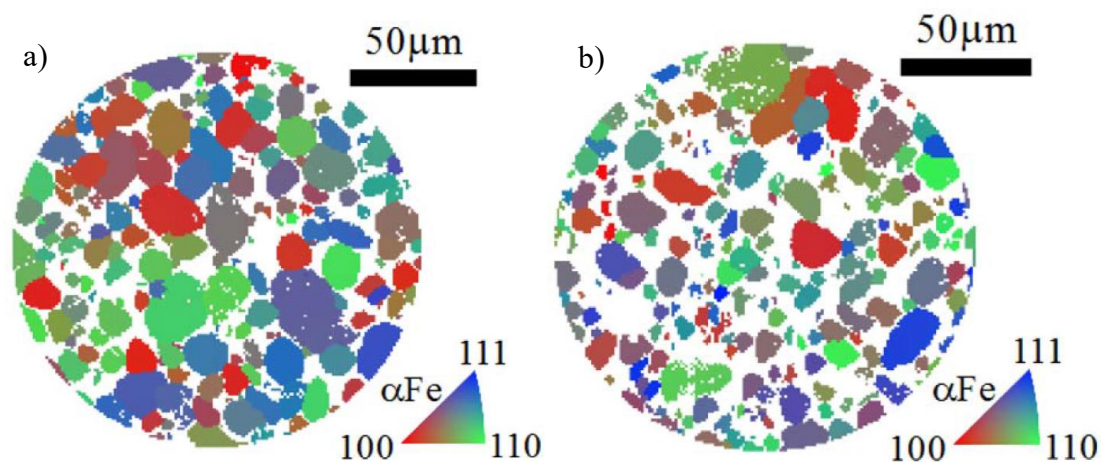


Fig. 5. Non-destructive crystal orientation mapping of (a) carbon steel S35C and (b) S45C.